Published in final edited form as:
*Cytotherapy*. 2013 January ; 15(1): 20–32. doi:10.1016/j.jcyt.2012.10.003.

# Tumor Stroma Engraftment of Gene-Modified Mesenchymal Stem Cells as Anti-Tumor Therapy against Ovarian Cancer

**Jennifer L. Dembinski**[*,1], **Shanna M. Wilson**[*,1], **Erika L. Spaeth**[*,1], **Matus Studeny**[1], **Claudia Zompetta**[1,2], **Ismael Samudio**[1,4], **Katherine Roby**[3], **Michael Andreeff**[1], and **Frank C. Marini**[1,†]

[1]Department of Leukemia, The University of Texas M. D. Anderson Cancer Center, Houston, TX USA

[2]Experimental Medicine and Pathology, University of Rome La Sapienza, 00185 Rome, Italy

[3]Center for Reproductive Sciences and Department of Anatomy and Cell Biology, University of Kansas Medical Center, Kansas City 66160, USA.

[4]Cellular and Molecular Therapy Group, Pontificia Universidad Javeriana, Bogotá, Colombia

## Abstract

Many ovarian cancers originate from ovarian surface epithelium, where they develop from cysts intermixed with stroma. The stromal layer is critical to the progression and survival of the neoplasm and consequently is recruited into the tumor microenvironment. Using both syngenic mouse tumors (ID8-R), and human xenograft (OVCAR3, SKOV3) tumor models, we first confirmed intraperitoneally-circulating MSC could target, preferentially engraft and differentiate into α-SMA+ myofibroblasts, suggesting their role as “reactive stroma” in ovarian carcinoma development and confirming their potential as a targeted delivery vehicle for the intratumoral production of interferon-beta (IFNβ). Then, mice with ovarian carcinomas received weekly IP injections of IFNβ expressing MSC, resulting in complete eradication of tumors in 70% of treated OVCAR3 mice ($P = 0.004$) and an increased survival of treated SKOV3 mice compared with controls ($P = 0.01$). Similar tumor growth control was observed using murine IFNβ delivered by murine MSC in ID8-R ovarian carcinoma. As a potential mechanism of tumor killing, MSC produced IFNβ induced caspase-dependent tumor cell apoptosis. Our results demonstrate that ovarian carcinoma engraft MSC to participate in myofibrovascular networks and that IFNβ produced by MSC intratumorally modulates tumor kinetics, resulting in prolonged survival.

### Keywords

mesenchymal stem cell; MSC; gene therapy; ovarian carcinoma; beta-interferon; ID8; non-invasive imaging

[†]To whom correspondence and reprint requests should be addressed at his current institution: Wake Forest University, Institute for Regenerative Medicine Comprehensive Cancer Center, fmarini@wakehealth.edu.
[*]all 3 authors contributed equally to this work.

## Introduction

Ovarian cancer claims the highest mortality rate of all gynecologic tumors. Women with ovarian cancer have a 10 year survival rate of 38%. [1] Ovarian cancer rarely metastasizes outside the abdominal cavity, but once an ovarian cell undergoes neoplastic transformation, it freely disseminates throughout the peritoneal cavity.[2] The low rate of survival is due primarily to two factors: 1) the advanced stage of the disease at diagnosis and 2) the limited efficacy of available therapeutic options. It is therefore essential that novel therapies be developed for this cancer.

Typically, the inclusion cysts from which most ovarian cancers develop a local solid intra-abdominal tumor in which there is a clear border between the tumor cells and the host stroma. [3] The stromal tissues appear to be required for tumor progression; providing structural support for the malignant cells, influencing vasculogenesis, and regulating the phenotypic behavior of the cancer. In turn, ovarian tumors provide growth factors, cytokines, and additional cellular signals that continually initiate new stromal reactions and recruit new cells into the tumor microenvironment that further support tumor growth. One cell type that could respond to tumor-produced signals and be recruited into growing tumors are mesenchymal stem cells/mesenchymal stromal cells (MSC).

MSC are nonhematopoietic, multipotent cells that contribute to the maintenance and regeneration of connective tissues including wounds and tumors.[4,5] Interestingly, the microenvironment in which solid tumors grow and develop resembles the cellular milieu that develops during wound healing or tissue damage/repair. This is potentially due to increased cell turnover, the tissue remodeling, and/or the production of appropriate paracrine signals that accompany wound healing. [6] Although not yet fully elucidated, MSC migration towards and engraftment in the tumor microenvironment is mediated by the inflammatory mediators produced within that microenvironment.[7,8,9] We and several other groups have shown the potential use of MSC for cellular therapy applications.[10-14,43]

Interferon-beta (IFNβ) is a cytokine with pleiotropic effects, including the inhibition of tumor growth and metastasis. [15,16] IFNβ also has pro-apoptotic effects on many types of malignant cells *in vitro*.[17-19]However, recombinant IFNβ has performed poorly in clinical trials to treat solid tumors due to its short biological half-life[20-23] and dose related toxicities. [24,25] Therefore the systemic administration of recombinant IFNβ has not produced adequate drug levels to eradicate tumors.[16,26] In contrast, potent antitumor effects have been demonstrated in animal models when IFNβ has been secreted via viral vectors intratumorally. [27,28] Given the similarity between wound healing and ovarian carcinoma-induced stromal response [6], we tested the hypothesis that ovarian carcinomas would recruit circulating MSC to participate in their stroma development and that these MSC could be used as a means of achieving intratumoral therapy.

Herein our data suggests that ovarian tumors selectively engraft exogenously injected MSC circulating within the intraperitoneal cavity that subsequently participate in the tumor myofibroblast networks. Furthermore, when gene-modified MSC-IFNβ engraft, they produce IFNβ intratumorally at levels sufficient to inhibit growth of ovarian tumors in both syngenic murine and human tumor xenograft models.

## Results

### IFNβ Inhibits Proliferation of Ovarian Cancer Cells *in Vitro*

Recombinant IFNβ protein and IFNβ-expressing MSC (MSC-IFNβ) inhibited the proliferation of ovarian carcinoma cells *in vitro* in a concentration-dependent manner (Fig.

1). Human OVCAR3 cells were most sensitive to human IFNβ (inhibitory concentration 50% [$IC_{50}$] = 5 IU/ml; Fig. 1A): these cells were approximately 20 times more sensitive than SKOV3 cells ($IC_{50}$ = 100 IU/ml, Fig. 1C) and approximately 200 times more sensitive than HEY cells ($IC_{50}$ = 1000 IU/ml; Fig. 1E). The murine ovarian carcinoma cell line (ID8-R), was also inhibited at an $IC_{50}$ of 50 IU/ml (Fig. 1G), utilizing murine IFNb. Both OVCAR3 and SKOV3 cells also showed evidence of apoptosis, as determined by propidium iodide staining, and inhibition of proliferation (data not shown). These *in vitro* results were consistent with the results obtained from coculture of human MSC-IFNβ with OVCAR3, SKOV3, and HEY cells or murine MSC-IFNβ with ID8R cells (Fig. 1B, 1D, 1F and 1H respectively).

### IFNβ half-life and toxicity *in vivo*

Plasma IFNβ levels after IP injections of recombinant IFNβ (40,000 IU) confirmed its short biological half-life with peak plasma levels of IFNβ decreasing 2 hours post injection and undetectable after 24 hours. However, after IP injection of MSC-IFNβ, IFNβ was detectable systemically at >5 IU/ml for up to 6 days (Fig. 2A). These data demonstrate that a single IP injection of MSC-IFNβ can generate systemic IFNβ levels for extended periods *in vivo*. To ensure that 5 IU/ml of IFNβ was a non-toxic level of IFNβ to mice, we injected 30 IU of murine IFNβ for 10 consecutive days into 5 mice and grossly observed the mice. During this treatment, the mice exhibited no outward signs of toxicity (fur ruffling, hunched posture, anorexia, wasting; data not shown).

### Mechanisms of IFNβ based killing

To determine a potential mechanism of how MSC-produced IFNβ controls tumor growth in ovarian cancer cells *in vitro*, OVCAR3 (Fig. 2B) or SKOV3 (Fig. 2C) cells were co-cultured with MSC-IFNβ, recombinant IFNβ protein or MSC alone in the presence or absence of a pan-caspase inhibitor. Apoptotic ovarian cancer cells are characterized as having decreased tetramethyl rhodamine methyl ester (TMRM) fluorescence, and increased Annexin V–FLUOS staining is displayed as a percent of positive control. TMRM fluorescence defined the change in mitochondrial dysfunction that accompanies cytochrome c release during apoptosis and detection of externalization of phosphatidyl serine by Annexin V defined early apoptosis. In OVCAR3 and SKOV3 cells co-cultured with MSC-IFNβ or treated with recombinant IFNβ, apoptosis increased over 48 hours (OVCAR3 45-80%; SKOV3 37-67%). In ovarian carcinoma cells cultured with MSC (control) or alone (without IFNβ), apoptosis was less than 10%. When OVCAR3 or SKOV3 were cultured with IFNβ and caspase inhibitors, apoptosis was blocked for 48 hours (<5%). These results suggest that caspase activation is an important part of apoptosis in ovarian cancer treated with IFNβ, in the absence of a significant immune component.

### Ovarian carcinomas selectively engraft intraperitoneally circulating MSC

To investigate if established ovarian tumors would engraft gene-modified MSC, we injected mice IP with five once weekly dose of $5\times10^5$ MSC-βgal (× 5 weeks), and their localization was traced histochemically utilizing X-gal staining. One group of mice had established abdominal OVCAR3 (n=5) or SKOV-3 (n=5) (Fig. S2a-d) tumors initiated 15 days prior. As a control, normal SCID mice without tumors (n=3) were injected with MSC-βgal. IHC was performed 14 days after the last dose of MSC-βgal was administered (49 days after the first MSC injection). As shown in Figs. S2e-h, representative sections from ovarian tumors display X-gal-positive colonies (1-3 colonies per field) that were incorporated into the tumor architecture. When MSC-βgal was injected IP into animals bearing OVCAR3 or SKOV3 tumors, there were no X-gal positive cells in the remaining tissues (spleen, kidney, muscle; Fig. S2i) Taken together, these results suggest that if MSC do engraft in normal tissues or

organs, it is below our limit of detection, whereas engraftment of MSC into the tumor microenvironment was robust.

### Fate of tumor resident MSC

To determine the fate of tumor engrafted MSC, we surveyed tumors from animals that received MSC. IHC staining for, human α-smooth muscle actin, human desmin, FSP, or FAP (Fig. 3) was performed on 82-day-old SKOV3 tumors of mice that had received five IP injections (1× per week) of 1 million MSC. Most $CD105^+$ (undifferentiated) MSC were detected on the periphery of the tumor, forming an encapsulating network. In contrast, MSC within and throughout the tumor became positive for α-SMA and desmin, exhibiting characteristics of smooth muscle-like myofibroblast cells that participate in fibrovascular networks. FSP, and/or FAP expression also identifies activated fibroblasts within the tumor microenvironment that has been infiltrated by reactive stroma.

### MSC-IFNβ Modulate Tumor Growth in Xenograft Mouse Model *In Vivo*

Once it was demonstrated that MSC would engraft in established ovarian tumors, we tested the efficacy of MSC-IFNβ *in vivo*, utilizing a SCID mouse xenograft model. Ovarian carcinomas were established by IP injection of OVCAR3 ($5\times10^6$) or SKOV3 ($6\times10^6$) cells) and 15 days later, $5\times10^5$ MSC-IFNβ (n=10) were administered IP once per week for five weeks. Control animals received once weekly (×5) IP injections of $5\times10^5$ MSC-βgal (n=5), or no injections (tumor only) (n=5). The animals were monitored until death, and the differences in overall survival were analyzed by log-rank test. In mice bearing established OVCAR3 xenografts, five once weekly treatments with MSC-IFNβ not only controlled tumor growth but significantly extended survival (p=0.03; Fig. 4A) as compared with OVCAR3 control mice (p=0.01). In fact, in 70% (7/10) of OVCAR3 mice, we were unable to detect any tumor development after MSC-IFNβ treatment. These mice remained tumor free for 169 days, at which point, the remaining 7 mice were sacrificed and evaluated for evidence of disease. Although no residual disease was detected, we cannot decisively claim that the tumor was completely eradicated. In mice bearing established SKOV3 xenografts, five once per week injections of MSC-IFNβ also inhibited tumor growth and significantly prolonged survival (p=0.001), as compared with control SKOV3 tumor-bearing animals alone (p=0.01) (Fig. 4B). These results correlate strongly with the *in vitro* sensitivity of OVCAR3 cells to IFN-β.

### Detection of IFNβ secreted by MSC in ovarian tumors

Immunohistochemical staining for IFNβ was performed on OVCAR and SKOV3 (Fig. 4C) tumors 1 or 3 days after IP injection of MSC-IFNβ. Strongly positive staining in the tumors, just 1 day after MSC-IFNβ injection, was detected. Interestingly, a 20-24 -fold increase in the levels of IFNβ production (OVCAR3 2.6-63%; SKOV3 2.1-43%) on day 3 was observed and associated with intense staining throughout the entire tumor. This observation suggests an increase in localized MSC after 3 days leading to an increase in total IFNβ production within the tumor microenvironment.

### Murine MSC-IFNβ Modulate Tumor Growth in syngenic Mouse Model *In Vivo*

Next, we tested whether murine ovarian tumors would selectively recruit circulating gene-modified murine MSC (mMSC) as stromal precursors, and whether these cells could also control tumor progression, similar to what we observed in the xenotransplant models. We therefore utilized a syngenic mouse model whereby immunocompetent C56Bl/6J mice bearing ID8-R, a murine ovarian carcinoma stably expressing renilla luciferase, were treated with either murine MSC expressing murine IFNβ (mMSC-mIFNβ; n=5) or mMSC expressing firefly luciferase (mMSC-ffLuc; control cells; n=5) or murine-derived mouse

embryomic fibroblast expressing firefly luciferase (C56Bl/6J MEF; n=3). We labeled all mMSC with firefly luciferase to facilitate non-invasive detection of biodistribution and engraftment into the tumor. By utilizing selective substrates, one can visualize either ID8-R tumor (renilla luciferase) or mMSC (firefly luciferase) in co-localization or as disparate entities. As shown in Fig. 5, both established ID8-R tumors or mMSC were readily detected in mice, and treatment of ID8-R tumors with mMSC-mIFNβ resulted in a significant reduction (1 log) of tumor-associated bioluminescence at day 53 over that of ID8-R treated with mMSC-ffLuc as determined by IVIS (Fig. 5A and 5C). Importantly, bioluminescence from both ID8-R and mMSC co-localized in tumor-bearing mice, as visualized by bioluminescence imaging (BLI; Figs. 5C,5D, and 5F), but we observed a random distribution of MEFs throughout the abdomen, with no specific association with the tumor bioluminescence (Fig. 5F). These data were further validated by IHC staining of the ID-8R tumors for ffLuc confirming the presence of labeled mMSC within the tumor whereas labeled-MEFs were not selectively localized to the tumor (data not shown). The BLI photon counts were graphed over time to show the ID8R tumor progression by luminescence compared to the tumor progression of the mice receiving the MSC-βgal or MSC-IFNβ. Immediately following the onset of IP MSC-IFNβ injection, the BLI decrease significantly compared to the controls (Fig. 5E).

Taken together, these data suggest that both hMSC and mMSC preferentially engraft in their respective tumor microenvironments. Thus the MSC deliver species-specific mIFNβ locally to the tumor microenvironment, resulting in reduction of tumor size and prolonged survival.

## Discussion

Our study demonstrates that ovarian carcinomas selectively recruit intraperitoneally circulating MSC to participate in stroma formation, and when armed to secrete interferon-beta, MSC effectively control or eradicate ovarian tumors in both syngenic and xenograft tumor models. Epithelial derived ovarian tumors grow as a solid mass or in a cyst formation as spheroids and typically disseminate intra-abdominally through the intraperitoneal fluid or ascites. [29] Upon IP administration of the Skov-3 tumor cell line, and in evaluating the recruitment of MSC during ovarian carcinoma growth, we found the stromal compartment of ovarian tumors colonized by exogenously administered MSC. These findings suggest that the recruitment and incorporation of exogenously administered MSC into the architecture of human ovarian carcinomas are important, selective phenomena that target a unique microenvironment and not homeostatic host tissues. Furthermore, MSC recruitment into the tumor microenvironment was efficient, with multiple colonies of MSC-βgal present within each microscopic field. Our whole-mount observations and histologic analyses further demonstrate that normal tissues did not exhibit any IHC detectable MSC incorporation, whereas multiple small tumor masses dispersed throughout the peritoneum were positive for MSC. Indeed, Komarova et al. demonstrated “preferential homing” of mesenchymal progenitor cells (MPC), a potentially similar stem cell, into xenotransplanted tumors in SCID mice, while observing no engraftment in normal organs. [13]

In our mouse models, we determined that tumor-resident MSC were capable of maintaining a constant low-level production of IFNβ locally at the tumor site for at least 6 days as compared to the rapid clearance of the IFNβ from the high therapeutic doses of INFβ IP which is confirmed by previous studies.[44] Although we detected low non-therapeutic serum levels of IFNβ (10 IU or lower) in the plasma, higher concentrations of IFNβ were most likely present intratumorally, exerting antitumor efficacy. Of importance, the low levels of detectable systemic IFNβ had minimal biological toxicity in mice, as mice receiving daily IP injection of murine IFNβ (30 IU/ML) displayed no signs of toxicity, such as fur ruffling, hunched posture, diarrhea (data not shown), similar to what we observed in prior studies

using systemically delivered MSC-IFNβ in xenograft melanoma and breast tumor models. [11,30] On days 1 and 3 post injection we observed, by IHC and bioluminescence imaging, MSC incorporation into the tumor. The tumor-resident MSC-IFNβ were capable of engulfing the entire tumor with IFNβ. Our data appear to be consistent with the findings of Odaka et al.,[31] who showed that the expression of IFNβ in a very small fraction of tumor cells (< 5%) completely prevented the IP development of ovarian tumors.

Because of a possible biological bias of the human xenograft model (human MSC engrafting in human tumors only and not in murine tissue), we utilized a syngenic murine ovarian tumor model. Murine MSC secreting muIFNβ selectively engrafted in murine ID8-R tumors, whereas syngenic fibroblasts displayed no selectivity for tumors. Importantly, mMSC-mIFNβ was effective at controlling ID8-R tumor growth *in vivo*, without detectable evidence of engraftment in other normal organs and tissues. Prior reports utilizing PCR to detect gene labeled MSC after IV injection suggest that very low or no engraftment of MSC occurred in normal tissues but increased dramatically only after tissue damage. [32] Similarly, we observed no MSC engraftment in normal tissues and only in the tumor, further supporting previous evidence that the tumor microenvironment is directly responsible for selectively engrafting MSC, be it murine MSC to murine tumors, or human MSC to human tumors.

We also determined the fate of tumor resident MSC after engraftment into the tumor microenvironment. Two interesting points bear out from this data: a) MSC that engraft externally along the periphery of the tumor remain undifferentiated, yet form complex encapsulating networks surrounding the tumor, while b) MSC migrating inward and throughout the tumor appear to differentiate into α-SMA+, desmin+ myofibroblast-like cells. These cells form elongated “streams” of cells that interdigitate throughout the tumor. Recent evidence suggests that SMA+ stromal fibroblasts contribute to the fibrovascular or perivascular networks during angiogenesis in developing tumors.[33] The tumor-incorporated MSC from the experiments described herein could also be participating in similar networks.

We were able to observe the variability of IFNβ-delivered by MSC in multiple *in vivo* tumor models, allowing us to observe a robust response in sensitive tumor models such as the OVCAR3 and more aggressive tumor models such as the syngenic ID8R. In all models, MSC were capable of producing an effective dose of IFNβ that elicited a tumor growth response and a survival advantage to the MSC-IFNβ treated mice. There are discrepancies between the tumor models in the survival advantage of the mice that received the MSC-βgal control cells. Klopp *et al* composed a thorough review in 2011 of manuscripts showing the promotion or inhibition of tumor growth by MSC.[45] In concordance with the review, one of our human tumor models shows an *in vivo* survival advantage with control MSC and the other does not. This discrepancy between models may be due to the tumor response to MSC paracrine stimulation in a xenograft environment. The variation in our data exemplifies the heterogeneity that exists in the patient population and serves as a reminder of disparity that exists in the clinical application of novel therapeutic agents.

While the mechanisms by which IFNβ induces apoptosis are not completely understood, a recent report suggested that IFNβ directly activates the extrinsic apoptosis pathway in cancer cells, and this effect depends on the expression of interferon receptors.[34] Our results, indeed suggest a critical role for caspase activation in the induction of ovarian cancer cell apoptosis by IFNβ as evidenced by the ability of the pan-caspase inhibitor, N-Benzyloxycarbonyl-Val-Ala-Asp(O-Me) fluoromethyl ketone (z-VAD-FMK), to prevent loss of $\Delta\Psi M$ and externalization of phosphatidyl serine. Interestingly, production of TRAIL has recently been shown to mediate the cytotoxic effects of IFNβ in ovarian cancer cells in culture [35], suggesting a possible mechanism by which IFNβ producing MSC induce

apoptosis of ovarian cancer cells in the absence of active immunity. In addition, IFNγ cooperates with 5-aza-cytidine in sensitizing cells to TRAIL inducing apoptosis by upregulating caspase 8 [36], and INFα can mediate induction of TRAIL by human monocytes.[37] Together these data suggests that the extrinsic apoptotic pathway contributes in large part to the direct cytotoxic effects of the interferons, in the presence or absence of active immunity. Future studies are aimed at elucidating the precise mechanisms by which IFNβ-producing MSC induce apoptosis in ovarian cancer tumors *in vivo*.

One possible bias in this study was that the sensitivities of the different ovarian carcinoma cells to IFNβ might have affected the cure fraction of our *in vivo* experiments. Each tumor cell type exhibited a slightly differing sensitivity to IFNβ and these differential sensitivities may involve the *p53* status of the cells. IFNβ has been shown to boost the transcription of the *p53* gene and increase its protein levels.[38] OVCAR3 cells, which express a mutated *p53* gene (with a point mutation at codon 248), were very sensitive to IFNβ, whereas SKOV3 cells, which do not express *p53*, were less sensitive. In a study of cisplatin cytotoxicity investigators saw no differences in growth inhibition between *p53* wild type compared to *p53* mutant ovarian cancer cell lines. [39] Thus, the p53 status of the OVCAR3 cells may have a role in the increased sensitivity to IFNβ leading to the complete eradication of tumors in a large percentage of OVCAR3 xenograft mice. Future studies need to be performed to address this question specifically.

We [11,30] and others[13,40,41,43] have demonstrated that MSC can be used as anti-tumor vehicles delivering oncolytic viruses, suicide genes, IL-21 and IFNβ against multiple tumor types. These data demonstrate a comparison between a fully syngenic model and a human xenotransplant tumor model where we describe a striking similarity between the two models in which both clearly demonstrate that MSC migrate to and selectively engraft into growing ovarian tumors, and control tumor growth using IFNβ. Additionally, use of noninvasive imaging has allowed us to display significant colocalization of MSC and tumor *in vivo*, whereas control fibroblasts are randomly dispersed throughout the intraperitoneal cavity. These data further demonstrate and reinforce the unique property of MSC to engraft at sites of tissue remodeling-ie the tumor, and not in surrounding homeostatic tissues.

In conclusion, ovarian tumors possess microenvironments conducive to MSC engraftment. Therefore, exploiting the innate ability of MSC to selectively engraft in these tumors is a promising approach to ovarian cancer therapy; clinical trials testing this approach are currently underway.

## Methods & Materials

### Cell isolation and culture

Human MSC were isolated as previously described [24]. Human ovarian cancer OVCAR cells were a gift from Dr. Judith K. Wolf (Department of Gynecologic Oncology, The University of Texas M. D. Anderson Cancer Center, Houston, TX). The cells were maintained in Roswell Park Memorial Institute medium (RPMI-1640) supplemented with 10% fetal bovine serum (FBS), L-glutamine, and a penicillin-streptomycin mixture (Gibco/Invitrogen, Carlsbad, CA). Human ovarian cancer SKOV3 cells were obtained from the American Type Culture Collection (Manassas, VA) and cultured in minimal essential medium Earl's salts with nonessential amino acids (supplemented with 10% FBS, L-glutamine, and a penicillin-streptomycin mixture). Human ovarian cancer HEY cells were also obtained from the American Type Culture Collection and cultured in RPMI-1640 supplemented with 10% FBS, L-glutamine, and a penicillin-streptomycin mixture.

Murine ID8 ovarian tumors: ID8, a cell line derived from spontaneous *in vitro* malignant transformation of C57BL/6J mouse ovarian surface epithelial cells were obtained from Dr. Katherine Roby[42], and were maintained in Dulbecco's modified Eagle's medium (Invitrogen, Carlsbad, CA) supplemented with 4% fetal bovine serum, 100 U/ml penicillin, 100 g/ml streptomycin, 5 g/ml insulin, 5 g/ml transferrin, and 5 ng/ml sodium selenite (Roche, Indianapolis, IN) in a 5% CO2 atmosphere at 37° C. These cells were stably infected with a lentivirus expressing renilla luciferase (RENLuc) and GFP [33]. Post-transfection GFP+ ID8 (ID8-R) cells were enriched by FACS (98% GFP+), grown to confluence, and used in subsequent experiments.

Murine MSC: Male, C57BL/6J, mouse marrow stromal cells (mMSC) were obtained from Darwin Prockop (Tulane University, New Orleans, LA). mMSC were cultured in alpha MEM with 10% horse serum, 10% fetal calf serum and supplemented with 10% FBS, L-glutamine, and a penicillin-streptomycin mixture. Passages 5-8 were used throughout this experiment. C57BL/6J MEFs were isolated from mice embryos using standard methods.

### Adenoviral vectors and MSC transduction

Ad-IFNβ was created as previously described [24]. Fiber modified adenoviruses expressing either murine IFNβ (AdmIFNβ-F/K21) or firefly luciferase (Ad-FF/luc-F/K21) were generated as described in Yotnda et al [34]. mMSC were incubated with adenoviruses at 50 viral particles/cell (based on OD reading) for 4 hours, after which fresh media was applied. The next day mMSC were assessed for transgene production. For Ad-IFNβ 50vp/cell resulted in the production of $4\times10^4$ IU IFNβ per $5\times10^5$ MSC after 24 hours. For Ad-mIFNβ, 50vp/cell resulted in production of 5 IU muIFNβ/ per $1\times10^6$ MSC after 24 hours. Firefly luciferase (FFLuc) expression was determined by addition of 2ul of a 40mg/ml stock solution D-Luciferin (Xenogen Co, Temecula CA) in 1 ml of media. Cells were visualized and quantitated by the Xenogen 100 IVIS. β-gal expression was determined by histochemical staining, and >90% of MSC were X-gal positive.

### In vitro proliferation assay

Cell monolayers were washed with PBS, harvested with trypsin EDTA, and resuspended in the appropriate medium as described previously. Cells were plated at a density of 1000 (HEY & ID8-R), 3000 (SKOV3) or 4000 (OVCAR3) cells per well (on the basis of their growth rate) in 200 μl of medium. Cells were allowed to adhere to the plate overnight, after which human IFNβ (Avonex, Biogen Inc.) or murine IFNβ (mIFNβ; ID8-R cells) (Biosource, Camarillo, CA) was added to the plate in different dilutions (range from 0-10,000 IU). One plate was read by MTS (Promega Inc., Madison, WI) assay at the time of initial addition of IFNβ, to serve as the initial control. Eight wells were used for each dilution of IFNβ. Medium was changed daily, and after five days, the assay was read using MTS. Absorbance was measured at 490nm. Results were calculated as follows: relative proliferation = ($OD_{IFNb}$ / $OD_{CNT}$) where $OD_{CNT}$ corresponds to $A_{490}$ of controls cells with no treatment, $OD_{IFNb}$ corresponds to wells treated with different concentrations of IFNβ for 5 days.

### In vitro co-culture of MSC with OVCAR3, SKOV3, and HEY

MSC were infected with an adenovirus carrying the IFNβ gene (MSC-IFNβ), to produce levels of 40,000 IU/$5\times10^5$ cells/ 24hours. Another flask of MSC was infected with an adenovirus carrying the beta-galactoside gene (MSC-ßgal), at levels to achieve >98% transfected cells. After 24 hours, cell monolayers were washed with PBS and removed using trypsin-EDTA; all cell lines were then resuspended in RPMI 1640 with 10% FBS. OVCAR3, SKOV3, or HEY cells were plated in 4 ml of medium either alone or mixed with MSC-IFNβ or MSC-βgal in a ratio of 1:1 or 10:1 respectively in six-well plates at a starting

concentration of $4 \times 10^4$ cells per well. After 5 days, cells were trypsinized, counted, and fixed with 70% ethanol. Cells were then labeled with PE (Sigma), and the cell DNA content was analyzed using the FACScan flow cytometer (Becton-Dickinson, San Jose, CA). The relative numbers of MSC (diploid cells) and ovarian carcinoma cells (aneuploid cells) were determined using ModFit software (Verity Software House Inc, ME).

### Mechanisms of IFNβ based killing

OVCAR3 or SKOV3 cells were co-cultured with MSC, MSC-IFNβ (created as previously stated), recombinant IFNβ or recombinant IFNβ with a pan-caspase inhibitor (1μM Z-VAD-FMK; R&D Systems, Minneapolis, MN) in 6 well transwell plates (Corning Inc., Corning, NY). Cells were incubated with either 1000 IU/ml/24 hours recombinant IFNβ, or with the appropriate number of MSC-IFNβ, which produced approximately 1000 IU/ml/24 hours of IFNβ. Negative controls were tumor cells alone, and positive controls were tumor cells with 10,000 IU/ml/24 hours recombinant IFNβ. Apoptosis was evaluated by two-color flow cytometry after staining the cells with the fluorescent mitochondrial potentiometric probe tetramethyl-rhodamine methyl ester (TMRM), and FITC-conjugated Annexin V. After treatment, cells were collected by trypsinization, washed twice in PBS and then resuspended in 100 μl of Annexin binding buffer (140 mM NaCl, 10 mM $KH_2PO_4$, 5 mM $CaCl_2$, pH 7.4) containing 25 nM of the mitochondrial potentiometric probe TMRM (Invitrogen, Carlsbad CA) and 1:100 dilution of Annexin V-FLUOS (Roche Diagnostics, Indianapolis IN) and incubated at 37°C for 30 min. Cells were washed in Annexin binding buffer and analyzed by flow cytometry in a FACS Calibur flow cytometer (FACScan; Becton-Dickinson, San Jose CA) using a 488 nm argon excitation laser. In this assay apoptotic cells display decreased TMRM fluorescence and increased Annexin V–FLUOS staining. Data is displayed as a percent of positive control.

### Animals, cell administration, non-invasive imaging of tumors and survival analysis

Female CB-17 SCID or C57BL/6J mice were purchased from Harlan (Indianapolis, IN) or Jackson Labs (Bar Harbor, ME) and used in accordance with institutional guidelines and under approved protocols. Tumors were created in the SCID or C57BL/6J mice by IP injection of either $5 \times 10^6$ OVCAR3, $6 \times 10^6$ SKOV3, or $5 \times 10^6$ stably expressing renilla luciferase ID8 (ID8-R) cells as a suspension in 1 ml of PBS. Survival durations were measured from the day of tumor cell injection until the day of death. Tumor imaging: tumors were imaged via IVIS (Xenogen 200 system, Caliper Life sciences, Hopkington MA). Mice with detectable tumors were used, and on day 25, the first of 5 (weekly) injections of $1 \times 10^6$ C57BL/6J mMSC expressed either FFLuc and mIFNβ (expressing ~ 5 IU/24h/million cells) (treatment group), or FFLuc alone (control group), or MEF expressing FFLuc (control group) IP. Bioluminescence (FFLuc detects mMSC or MEF and RENLuc detects tumor) activity was acquired and quantitated (1-2 minute collection time). Differences in survival were determined by a two-tailed log-rank test. Statistical analysis was performed with statistical software (Statistica; StatSoft, Tulsa, OK).

### Measurement of IFNβ concentration in mouse plasma

Mice with established ovarian tumors were injected with either $5 \times 10^5$ MSC-IFNβ IP or 40,000 IU of recombinant IFNβ IP. 200 μl of blood was collected in capillary tubes at appropriate time intervals. Mouse plasma was collected and utilized for determination of serum IFNβ levels (IFNβ-ELISA, Fujirebio Inc., Tokyo, Japan). The National Institutes of Health standard for IFNβ-1a was utilized to determine concentration.

### Tissue processing and imaging studies

Tumors and other organs were fixed in Bouin's solution or embedded in an ornithine transcarbamylase compound (OTC, Miles, Inc., Elkhart, IN), then snap-frozen in liquid nitrogen and stored at −80°C. Whole tumors from several animals were immediately examined for the presence of β-gal by using X-gal staining. Frozen tissue was sectioned (6–8 μm) and processed for hematoxylin-eosin or X-gal immunohistochemical staining. Photomicrographs were taken (Zeiss Axioplan2; Carl Zeiss, Inc., Thornwood, NY equipped with a charge-coupled device camera (Hamamatsu Corp., Bridgewater, NJ).

### X-gal histochemical staining

Whole tumors were fixed in 0.5% glutaraldehyde for 10 minutes and washed with PBS. Tissue was then incubated with a 2% X-gal solution (Sigma) with 1M $MgCl_2$, 30 mM potassium ferricyanide, and 30 mM potassium ferrocyanide overnight and refixed in 10% neutral-buffered formalin. Slides from frozen tissues were fixed with cold acetone/ethanol (1:1) for 20 minutes, stained with X-gal overnight, and counterstained with nuclear fast red.

### Immunohistochemical analyses

IFNβ, α-SMA or desmin was detected in frozen sections of the mouse tumors. Briefly, sections were fixed for 5 minutes in ph7 formalin, after endogenous peroxidase activity was quenched by incubating the sections in 0.3% hydrogen peroxide in methanol for 30 minutes. The sections were then treated with rabbit anti-IFNβ antibody (diluted 1:1000; Chemicon, Temecula, CA), mouse anti-human α-SMA (Biomeda Corp., Foster City, CA), or rabbit anti-human desmin (diluted 1:1000, Novus Biologicals, Littleton, CO) according to the procedures in the appropriate peroxidase kit (Vector Laboratories, Burlingame, CA). Peroxidase substrate was developed using the 3,3′-diaminobenzidine (DAB) or AEC (3-amino-9-ethylcarbazole) substrate kit (Vector Laboratories). Slides were then counterstained with hematoxylin (hematoxylin QS; Vector Laboratories), dehydrated, and either mounted with VectaMount Permanent Mounting Medium (Vector Laboratories) or mounted with a low-viscosity aqueous mounting medium (Scytek Laboratories, Logan, UT).

## Supplementary Material

Refer to Web version on PubMed Central for supplementary material.

## Acknowledgments

Supported in part by grants from the National Cancer Institute (CA-1094551, Ca-116199 RC1CA146381, P50CA083639, R01CA109451 and R01NS06994 for FCM, CA-55164, CA-16672, and CA-49639 for MA) and by the Stringer Professorship for Cancer Treatment and Research (MA). JLD, and FCM are supported in part by grants from the Susan G Komen Breast Cancer Foundation, the Ladies Leukemia League, and the W.M. Keck Foundation. ELS is supported in part by Army Department of Defense (BC083397).

## References

1. American Cancer SocietyCancer Facts & Figures 2009. American Cancer Society; Atlanta: 2009.
2. Kenny HA, Kaur S, Coussens LM, et al. The initial steps of ovarian cancer cell metastasis are mediated by MMP-2 cleavage of vitronectin and fibronectin. J.Clin.Invest. 2008; 118:1367–1379. [PubMed: 18340378]
3. Ghahremani M, Dorrington FoghiA. JHEtiology of ovarian cancer: A proposed mechanism. Med.Hypotheses. 1999; 52:23–26. [PubMed: 10342666]
4. Prockop DJ. Marrow stromal cells as stem cells for nonhematopoietic tissues. Science. 1997; 276:71–74. [PubMed: 9082988]

5. Pittenger MF, Mackay AM, Beck SC, et al. Multilineage potential of adult human mesenchymal stem cells. Science. 1999; 284:143–147. [PubMed: 10102814]
6. Dvorak HF. Tumors: wounds that do not heal. Similarities between tumor stroma generation and wound healing. N.Engl.J.Med. 1986; 315:1650–1659. [PubMed: 3537791]
7. Spaeth E, Klopp A, Dembinski J, et al. Inflammation and tumor microenvironments: defining the migratory itinerary of mesenchymal stem cells. Gene Ther. 2008; 15:730–738. [PubMed: 18401438]
8. Xu F, Shi J, Yu B, et al. Chemokines mediate mesenchymal stem cell migration toward gliomas in vitro. Oncol.Rep. 2010; 23:1561–1567. [PubMed: 20428810]
9. Coffelt SB, Marini FC, Watson K, et al. The pro-inflammatory peptide LL-37 promotes ovarian tumor progression through recruitment of multipotent mesenchymal stromal cells. Proc.Natl.Acad.Sci.U.S.A. 2009; 106:3806–3811. [PubMed: 19234121]
10. Studeny M, Marini FC, Zompetta C, et al. Bone marrow derived mesenchymal stem cells serve as precursors for stromal fibroblasts in malignant tumors and show potential for cancer therapy. Blood. 2001; 98
11. Studeny M, Marini FC, Champlin RE, et al. Bone marrow-derived mesenchymal stem cells as vehicles for interferon-beta delivery into tumors. Cancer Res. 2002; 62:3603–3608. [PubMed: 12097260]
12. Studeny M, Marini FC, Dembinski JL, et al. Mesenchymal stem cells: potential precursors for tumor stroma and targeted-delivery vehicles for anticancer agents. J.Natl.Cancer Inst. 2004; 96:1593–1603. [PubMed: 15523088]
13. Komarova S, Kawakami Y, Stoff-Khalili MA, et al. Mesenchymal progenitor cells as cellular vehicles for delivery of oncolytic adenoviruses. Mol. Cancer Ther. 2006; 5:755–766. [PubMed: 16546991]
14. Hata N, Shinojima N, Gumin J, et al. Platelet-derived growth factor BB mediates the tropism of human mesenchymal stem cells for malignant gliomas. Neurosurgery. 2010; 66:144–156. [PubMed: 20023545]
15. Wong VLY, Rieman DJ, Aronson L, et al. Growth-inhibitory activity of interferon-beta against human colorectal carcinoma cell lines. Int.J.Cancer. 1989; 43:526–530. [PubMed: 2494120]
16. Johns TG, Mackay IR, Callister KA, et al. Antiproliferative potencies of interferons on melanoma cell lines and xenografts: Higher efficacy of interferon β. J.Natl.Cancer Inst. 1992; 84:1185–1190. [PubMed: 1378904]
17. Chawla-Sarkar M, Leaman DW, Borden EC. Preferential induction of apoptosis by interferon (IFN)-β compared with IFN-α2: Correlation with TRAIL/Apo2L induction in melanoma cell lines. Clin.Cancer Res. 2001; 7:1821–1831. [PubMed: 11410525]
18. Chawla-Sarkar M, Lindner DJ, Liu Y, et al. Apoptosis and interferons: Role of interferon-stimulated genes as mediators of apoptosis. Apoptosis. 2003; 8:237–249. [PubMed: 12766484]
19. Zhang H, Koty PP, Mayotte J, et al. Induction of multiple programmed cell death pathways by IFN-β in human non-small-cell lung cancer cell lines. Exp.Cell Res. 1999; 247:133–141. [PubMed: 10047455]
20. Rambaldi A, Introna M, Colotta F. Intraperitoneal administration of interferon β in ovarian cancer patients. CANCER. 1985; 56:294–301. [PubMed: 2408731]
21. Kardamakis D. Interferons in the treatment of malignancies. In Vivo. 1991; 5:589–598. [PubMed: 1810444]
22. Cappelli R, Gotti G. The locoregional treatment of neoplastic ascites with interferon-beta. Recenti Prog.Med. 1992; 83:82–84. [PubMed: 1502425]
23. Einhorn S. Why do so many cancer patients fail to respond to interferon therapy? J.Interferon Cytokine Res. 1996; 16:275–281. [PubMed: 9162520]
24. Buchwalder P, Buclin T, Trinchard I, et al. Pharmacokinetics and pharmacodynamics of IFN-β1a in healthy volunteers. J.Interferon Cytokine Res. 2000; 20:857–866. [PubMed: 11054273]
25. Salmon P, Le Cotonnec J, Galazka A, et al. Pharmacokinetics and pharmacodynamics of recombinant human interferon- β in healthy male volunteers. J.Interferon Cytokine Res. 1996; 16:759–764. [PubMed: 8910759]

26. Johns TG, Kerry JA, Veitch BAJ, et al. Pharmacokinetics, tissue distribution, and cell localization of [$^{35}$S]methionine-labeled recombinant human and murine α interferons in mice. Cancer Res. 1990; 50:4718–4723. [PubMed: 2369745]
27. Pan J, Zhang M, Wang J, et al. Intratumoral injection of interferon-gamma gene-modified dendritic cells elicits potent antitumor effects: Effective induction of tumor-specific CD8$^{+}$ CTL response. J.Cancer Res.Clin.Oncol. 2005; 131:468–478. [PubMed: 15711825]
28. Streck CJ, Dickson PV, Ng CYC, et al. Adeno-associated virus vector-mediated systemic delivery of IFN-β combined with low-dose cyclophosphamide affects tumor regression in murine neuroblastoma models. Clinical Cancer Research. 2005; 11:6020–6029. [PubMed: 16115947]
29. Shield K, Ackland ML, Ahmed N, et al. Multicellular spheroids in ovarian cancer metastases: Biology and pathology. Gynecol.Oncol. 2009; 113:143–148. [PubMed: 19135710]
30. Studeny M, Marini FC, Dembinski JL, et al. Mesenchymal stem cells: potential precursors for tumor stroma and targeted-delivery vehicles for anticancer agents. J.Natl.Cancer Inst. 2004; 96:1593–1603. [PubMed: 15523088]
31. Odaka M, Sterman DH, Wiewrodt R, et al. Eradication of intraperitoneal and distant tumor by adenovirus-mediated interferon-β gene therapy is attributable to induction of systemic immunity. Cancer Res. 2001; 61:6201–6212. [PubMed: 11507073]
32. François S, Bensidhoum M, Mouiseddine M, et al. Local irradiation not only induces homing of human mesenchymal stem cells at exposed sites but promotes their widespread engraftment to multiple organs: A study of their quantitative distribution after irradiation damage. Stem Cells. 2006; 24:1020–1029. [PubMed: 16339642]
33. Spaeth EL, Dembinski JL, Sasser AK, et al. Mesenchymal stem cell transition to tumor-associated fibroblasts contributes to fibrovascular network expansion and tumor progression. PLoS ONE. 2009; 4:e4992. [PubMed: 19352430]
34. Saidi RF, Williams F, Ng J, et al. Interferon receptors and the caspase cascade regulate the antitumor effects of interferons on human pancreatic cancer cell lines. Am.J.Surg. 2006; 191:358–363. [PubMed: 16490547]
35. Morrison BH, Tang Z, Jacobs BS, et al. Apo2L/TRAIL induction and nuclear translocation of inositol hexakisphosphate kinase 2 during IFN-beta-induced apoptosis in ovarian carcinoma. Biochem.J. 2005; 385:595–603. [PubMed: 15634191]
36. Fulda S, Debatin K. 5-Aza-2′-deoxycytidine and IFN-γ cooperate to sensitize for TRAIL-induced apoptosis by upregulating caspase-8. Oncogene. 2006; 25:5125–5133. [PubMed: 16607283]
37. Gómez-Benito M, Balsas P, Bosque A, et al. Apo2L/TRAIL is an indirect mediator of apoptosis induced by interferon-α in human myeloma cells. FEBS Lett. 2005; 579:6217–6222. [PubMed: 16246331]
38. Takaoka A, Hayakawa S, Yanai H, et al. Integration of interferon-α/β signalling to p53 responses in tumour suppression and antiviral defence. Nature. 2003; 424:516–523. [PubMed: 12872134]
39. De Feudis P, Debernardis D, Beccaglia P, et al. DDP-induced cytotoxicity is net influenced by p53 in nine human ovarian cancer cell lines with different p53 status. Br.J.Cancer. 1997; 76:474–479. [PubMed: 9275024]
40. Matuskova M, Hlubinova K, Pastorakova A, et al. HSV-tk expressing mesenchymal stem cells exert bystander effect on human glioblastoma cells. Cancer Lett. 2010; 290:58–67. [PubMed: 19765892]
41. Sonabend AM, Ulasov IV, Tyler MA, et al. Mesenchymal stem cells effectively deliver an oncolytic adenovirus to intracranial glioma. Stem Cells. 2008; 26:831–841. [PubMed: 18192232]
42. Roby KF, Taylor CC, Sweetwood JP, Cheng Y, Pace JL, Tawfik O, et al. Development of a syngenic mouse model for events related to ovarian cancer. Carcinogenesis. 2000; 21:585–591. [PubMed: 10753190]
43. Hu W, Wang J, He X, Zhang H, Yu F, Jiang L, Chen D, Chen J, Dou J. Human umbilical blood mononuclear cell-derived mesenchymal stem cells serve as interleukin-21 gene delivery vehicles for epithelial ovarian cancer therapy in nude mice. Biotechnol Appl Biochem. 2011; 58:397–404. [PubMed: 22172102]
44. Rambaldi A, Introna M, Colotta F. Intraperitoneal administration of interferon β in ovarian cancer patients. CANCER. 1985; 56:294–301. [PubMed: 2408731]

45. Klopp AH, Gupta A, Spaeth E, Andreeff M, Marini F III. Concise review: Dissecting a discrepancy in the literature: Do mesenchymal stem cells support or suppress tumor growth? Stem Cells. 2011; 29:11–9. [PubMed: 21280155]

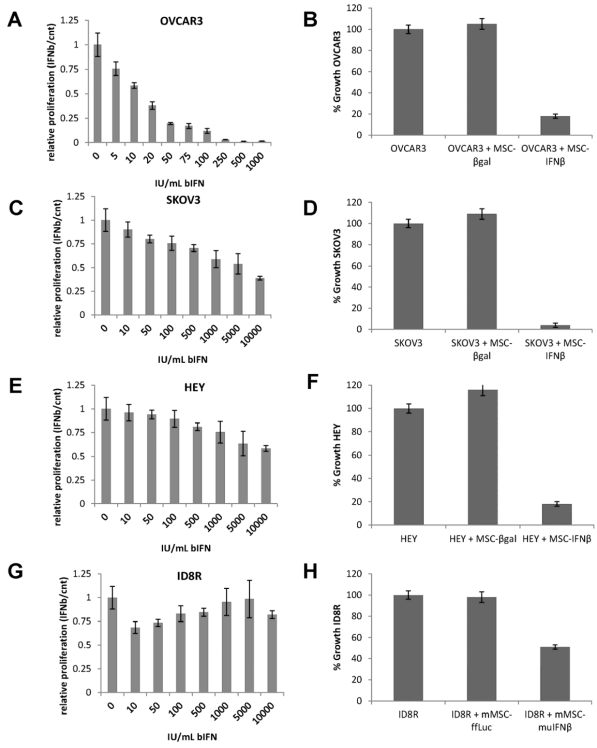


**Figure 1. IFNβ and MSC-IFNβ inhibit proliferation of ovarian carcinoma cells *in vitro***

(A) OVCAR3, (C) SKOV3, (E) HEY (G) ID8-R (C57BL/6J MOSEC, treated with murine IFNβ cells were cultured in the presence of increasing concentrations of IFNβ. The effect of IFNβ is expressed as proliferation relative to control cells that were not exposed to the IFNβ. Results are represented as the mean ± SEM. (B) OVCAR3, (D) SKOV3, (F) HEY and (H) ID8-R cells were co-cultured with MSC-βgal (mMSC-ffLuc for murine model) or MSC-IFNβ (mMSC-mIFNβ for murine model) in a 10:1 ratio. Cells were counted, and their relative number in co-cultures was determined by flow cytometry. Results (mean ± SEM) are expressed as the percentage of control cells (cultured alone).

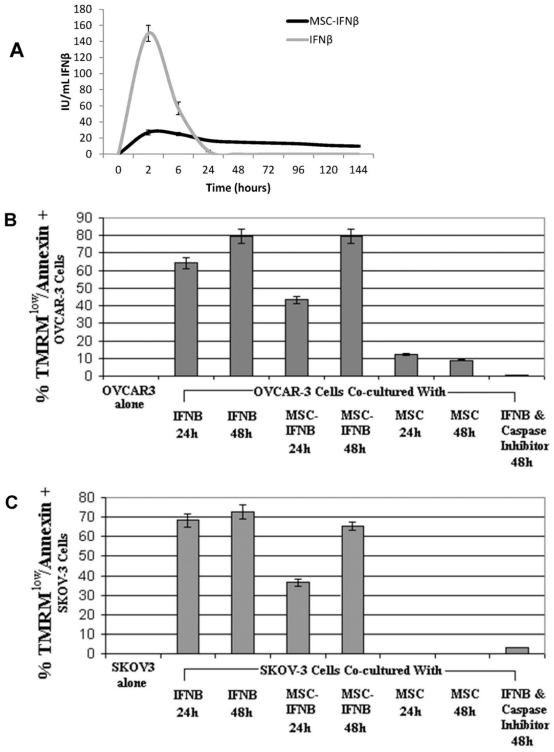


**Figure 2. Pharmacokinetics and mechanisms of IFNβ based killing**

(A) Determination of IFNβ serum levels after an IP injection of MSC-IFNβ (black line) versus an IP injection of 40,000IU IFNβ (grey line). After IP injection of $5\times10^5$ MSC-IFNβ blood was drawn at various time points and serum was assessed for IFNβ via ELISA. (B) OVCAR3 or (C) SKOV3 cells were co-cultured with MSC-IFNβ, recombinant IFNβ protein or MSC alone in the presence or absence of a pan-caspase inhibitor. Mitochondrial membrane potential ($\Delta\Psi M$) and externalization of phosphatydil serine were quantified by flow cytometery.

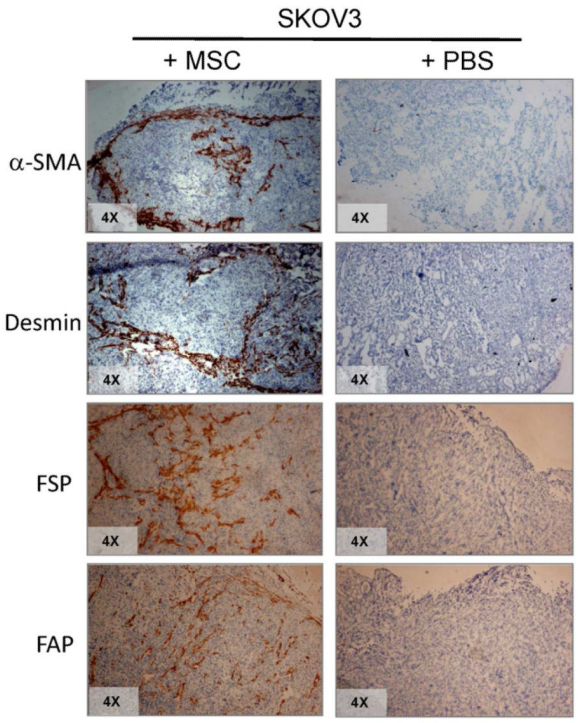


**Figure 3. Fate of engrafted MSC in the ovarian tumor microenvironment**

Fate of MSC engrafted in SKOV3 ovarian tumors *in vivo* was determined by immunohistochemistry on tumor sections. Frozen tissue sections harvested from day 82 ovarian carcinomas that were exposed to IP-circulating MSC or negative control ( IP injected PBS) were stained with human anti-α-smooth muscle actin and anti-desmin to show human myofibroblast incorporation within the tumor sections. FAP and FSP staining within the tumor sections depicts the activated fibroblasts within the tumor microenvironment. Dark red-brown staining indicates a positive result.

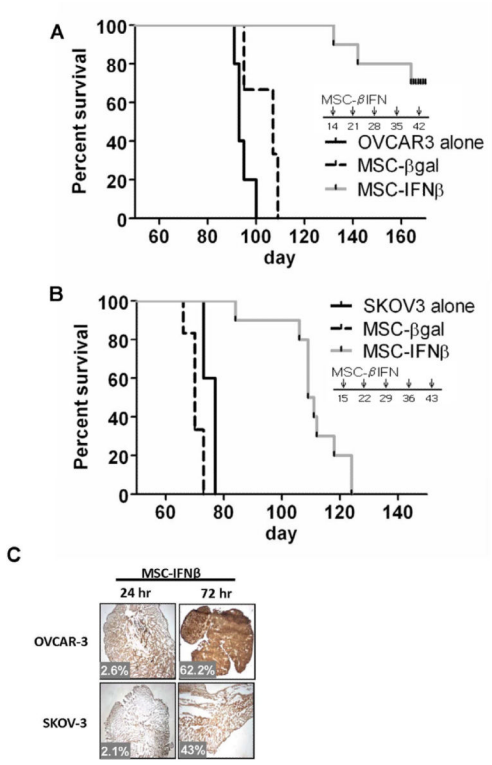


**Figure 4. IP administration of MSC-IFNβ significantly increases survival in mice with ovarian carcinomas**

Mice with established ovarian carcinomas (n=10 for each cell line) were treated with five once weekly IP injections of $5\times10^5$ MSC-IFNβ or MSC-βgal. (A) Kaplan-Meier survival curves for OVCAR3 mice. (B) Survival curves for SKOV3 mice. (C) To detect intratumoral IFNβ, OVCAR3 or SKOV3 tumor sections (10×) one and three days post IP injection of $1\times10^6$ MSC-IFNβ were stained with anti-IFNβ antibody as described in the methods. Dark red-brown staining indicates production of IFNβ by MSC. Densitometric quantitation of stained tumor sections was performed to assess levels of IFNβ production and integrated density values are displayed as percentage above background in the lower left corner of images.

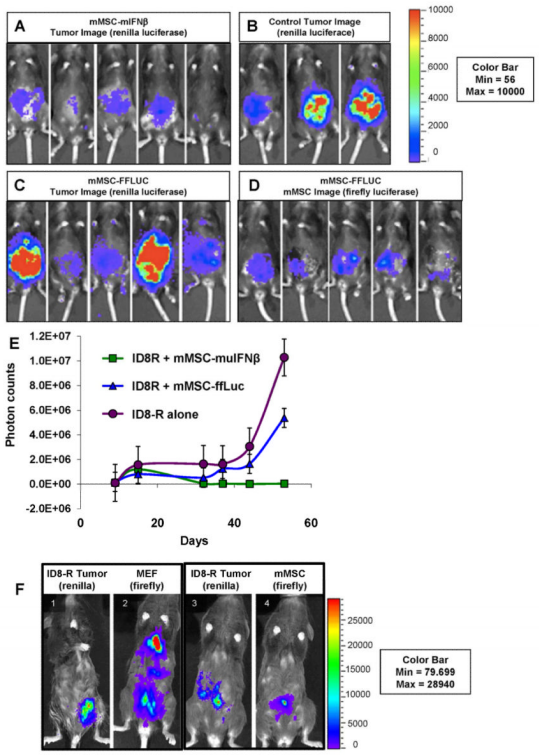


**Figure 5. Assessment of MSC engraftment and therapy for ID8-R ovarian carcinomas in a syngenic C56BL/6J mouse model by bioluminescent imaging**

BLI images of mice bearing ID8-R tumors: addition of renilla-specific substrate afford detection of ID8-R tumor, whereas addition of D-luciferin allows specific detection of firefly luciferase expressing mMSC. (A) Bioluminescence of ID8-R tumors (RENLuc) in mice that received 5 (1×/week) of $1\times10^6$ mMSC-mIFNβ at day 53. (B) Bioluminescence of ID8-R tumor (RENLuc) in control mice (no treatment-tumor alone) at day 53. (C) Bioluminescence of ID8-R tumor (RENLuc) in mice that received 5 (1×/week) of $1\times10^6$ mMSC-FFLuc (mMSC control) at day 53. (D) Detection of mMSC-FFLuc (Firefly-specific substrate) in mice that received 5 (1×/week) of $1\times10^6$ mMSC-ffLuc, taken on day 54, one day after panel C was imaged. (E) Tumor growth over time as assessed by average photon counts/tumor within each group shows a significant decrease in tumor size by BLI of the MSC-IFNβ treated mice compared to the control. (F) Detection of selected co-localization of either mMSC or mouse embryonic fibroblasts (MEF) in vivo. C56Bl/6J mice (n=5) with 58 days established ID8-R ovarian tumors (F-1, F-3) were injected with either $5 \times 10^5$ C56Bl/6J MEF(F-2) or mMSC (F-4). Mice were imaged on day 15 post-injection to detect either tumor (renilla-specific), or treatment (firefly-specific). A representative mouse from each group is shown.